

A POLYNOMIAL APPROXIMATION SCHEME FOR NONLINEAR MODEL REDUCTION BY MOMENT MATCHING*

CARLOS DOEBELI[†], ALESSANDRO ASTOLFI[‡], DANTE KALISE[†], ALESSIO MORESCHINI[‡], GIORDANO SCARCIOTTI[‡], AND JOEL SIMARD[‡]

Abstract. We propose a procedure for the numerical approximation of invariance equations arising in the moment matching technique associated with reduced-order modeling of high-dimensional dynamical systems. The Galerkin residual method is employed to find an approximate solution to the invariance equation using a Newton iteration on the coefficients of a monomial basis expansion of the solution. These solutions to the invariance equations can then be used to construct reduced-order models. We assess the ability of the method to solve the invariance PDE system as well as to achieve moment matching and recover the steady-state behaviour of nonlinear systems with state dimension of order 1000 driven by linear and nonlinear signal generators.

Key words. reduced-order modeling, moment matching, invariant manifolds, Galerkin methods, global polynomial approximation

AMS subject classifications. 49M15, 70Q05, 93A30

1. Introduction. Complex large-scale dynamical systems are ubiquitous in control engineering, providing a natural framework for modeling multi-agent systems, energy networks, and coupled electrical systems [25]. The high dimensionality of these models, often on the order of thousands or millions of states, introduces significant computational challenges, a phenomenon known as the “curse of dimensionality” [9]. Reduced-order modeling aims to alleviate this complexity while preserving important system characteristics. It finds application across many fields, including mechanical and electrical systems and weather forecasting [11, 2]. Broadly speaking, model order reduction methods are categorized as being based upon the singular value decomposition, such as Balanced Truncation [27, 26, 38] and Proper Orthogonal Decomposition [28, 29, 42], or upon Krylov projection/interpolation, such as moment matching [4, 3]; see [1] for a comprehensive overview. Other approaches include energy-based methods [16, 37], reduction around a limit cycle [17], and transfer function interpolation for polynomial systems [10].

In this paper, we consider potentially high-dimensional systems with a state $x(t) \in \mathbb{R}^n$, input $u(t) \in \mathbb{R}^m$, and output $y(t) \in \mathbb{R}^p$, governed by

$$\dot{x} = f(x, u), \quad y = h(x).$$

In particular, we are interested in the case where the input u is generated by an exogenous system with state $\omega(t) \in \mathbb{R}^d$, described by

$$\dot{\omega} = s(\omega), \quad v = \ell(\omega).$$

Under certain assumptions, the interconnected system obtained by setting $u = v$ admits a mapping $x = \pi(\omega)$ satisfying a system of first-order nonlinear partial differential equations (PDEs) known as the invariance equation, which characterizes an

*Revised manuscript submitted 27 March 2026.

[†]Department of Applied Mathematics, Imperial College London (c.doebeli22@imperial.ac.uk, d.kalise-balza@imperial.ac.uk)

[‡]Department of Electrical and Electronic Engineering, Imperial College London (j.simard18@imperial.ac.uk, a.moreschini@imperial.ac.uk, a.astolfi@imperial.ac.uk, g.scarciotti@imperial.ac.uk)

invariant manifold embedding the interconnected system’s dynamics. The goal of this work is to achieve nonlinear model reduction by moment matching by solving this invariance equation, yielding a reduced system with state $r(t) \in \mathbb{R}^d$ governed by

$$\dot{r} = \bar{f}(r, u), \quad y_r = \bar{h}(r),$$

whose output y_r approximates the steady-state behaviour of the full-order system under the same input. The precise mathematical setting is given in [Section 2](#).

For recent surveys on moment matching see *e.g.* [\[33, 36\]](#). For linear systems, moment matching is in one-to-one relation with the solution to a Sylvester equation induced by the interconnection of the system and the signal generator [\[15\]](#); with additional stability assumptions the invariant manifold is attractive and links to the steady-state response [\[21\]](#). This relationship was extended to nonlinear systems in [\[20\]](#), associating invariance with a “Sylvester-like” system of nonlinear coupled PDEs whose (locally) attractive solutions generalize the notion of steady-state response. Building on this, [\[4\]](#) generalized moment matching to nonlinear systems via the invariant manifold induced by the interconnection. Further developments include two-sided nonlinear moment matching [\[19\]](#), data-driven estimation via basis function fitting [\[35, 31\]](#), parametrization of all differential-algebraic interpolants [\[39, 40\]](#), and a closed-loop framework relaxing stability requirements [\[30\]](#). The notion of invariance also arises beyond model reduction, in output regulation [\[12\]](#) and in immersion and invariance control design [\[5\]](#).

The main limitation of the interconnection-based approach is the need to numerically solve a large-scale system of coupled nonlinear PDEs: for an n -dimensional system and a d -dimensional signal generator, this amounts to solving n PDEs over \mathbb{R}^d . In this paper, we propose a numerical scheme based on Newton’s method in conjunction with a global polynomial ansatz for each PDE solution. This approach, first explored for Hamilton-Jacobi-Bellman PDEs in [\[8, 7\]](#) and later extended to high-dimensional settings in [\[23, 22, 6\]](#), mitigates the curse of dimensionality at moderate computational cost. We focus on low-dimensional signal generators with $d = 2$ and high-dimensional dynamics with n up to 1000, a scale for which traditional grid-based PDE methods are impractical. The use of orthogonal polynomials for weighted residual methods in moment matching was explored in [\[14\]](#) for linear signal generators and low-dimensional dynamics.

1.1. Contribution. This paper focuses on the development of computational methods for nonlinear moment matching. The main contributions are as follows:

- We develop and implement a Galerkin method to find approximate solutions to the invariance PDE system and use these to construct reduced-order models achieving moment matching.
- The framework is tailored to nonlinear systems driven by low-dimensional signal generators, exploiting the interconnection structure to construct very low-dimensional reduced-order models that accurately reproduce steady-state behaviour and outperform standard model-order reduction (MOR) techniques at the same reduced order.
- This paper represents the first computational method explicitly developed for approximating the invariance equation in nonlinear moment matching. The method’s ability to handle systems with thousands of states is a key novel contribution.
- The method’s efficacy is demonstrated on systems of dimension up to 1000, systems driven by non-polynomial signal generator nonlinearities, and inter-

connected systems with implicitly defined nonlinear signal generators.

- The method applies beyond model order reduction, to output regulation and immersion and invariance problems.

1.2. Organization. The paper is organized as follows. In [Section 2](#) we give an overview of the problem setup and we show how moment matching is defined and how the invariance PDE system arises. [Section 3](#) introduces a Galerkin type method for the numerical computation of an approximate solution $\pi(\cdot)$ to the invariance PDE system. [Section 4](#) reports different numerical experiments assessing the accuracy of the proposed method and its effectiveness in generating a reduced-order model. [Section 5](#) discusses the results further and puts them in a wider context.

2. Moment Matching for Nonlinear Dynamical Systems. We consider dynamical systems with a state $x(t) \in \mathbb{R}^n$, an input $u(t) \in \mathbb{R}^m$, and an output $y(t) \in \mathbb{R}^p$, that can be represented in the form

$$(2.1) \quad \begin{aligned} \dot{x} &= f(x, u) \\ y &= h(x) \end{aligned}$$

We assume that the mappings $f : \mathcal{U} \times \mathcal{V} \rightarrow \mathbb{R}^n$ and $h : \mathcal{U} \rightarrow \mathbb{R}^p$ are C^2 , defined on open neighbourhoods $\mathcal{U} \subset \mathbb{R}^n$ and $\mathcal{V} \subset \mathbb{R}^m$ of the origin. We assume that system (2.1) has an equilibrium and, without loss of generality, that this equilibrium is satisfied at the origin, that is, $f(0, 0) = 0$ and $h(0) = 0$.

In order to introduce the notion of moment for a nonlinear system of the form (2.1), we consider the interconnection of (2.1) with an exogenous system, referred to as the *signal generator*, with a state $\omega(t) \in \mathbb{R}^d$ which is described by equations of the form

$$(2.2) \quad \begin{aligned} \dot{\omega} &= s(\omega), \\ v &= \ell(\omega), \end{aligned}$$

where $v(t) \in \mathbb{R}^m$ is the output of the signal generator system, and the mappings $s : \mathbb{R}^d \rightarrow \mathbb{R}^d$ and $\ell : \mathbb{R}^d \rightarrow \mathbb{R}^m$ are C^2 . We also assume that (2.2) has an equilibrium at the origin.

We denote by $\Xi_t^s : \mathbb{R} \times \mathbb{R}^d \rightarrow \mathbb{R}^d$ the flow generated by the vector field s , that is, the smooth function with the property that

$$(2.3) \quad \frac{\partial}{\partial t} \Xi_t^s(\omega_0) = s(\Xi_t^s(\omega_0)), \quad \Xi_0^s(\omega_0) = \omega_0.$$

Here, we introduce the notion of observability and accessibility, using the definitions introduced in [30], and based on [18] and [41]:

DEFINITION 2.1 (Observability). *The system (2.1) is said to be locally observable at the point x_0 if for every open neighbourhood U of x_0 , initial conditions $x_a(0) = x_0 \neq x_b(0) \in U$, and input $u(\cdot) \in L^\infty([0, \infty); \mathbb{R}^m)$ for which the corresponding trajectories $x_a(\cdot), x_b(\cdot)$ remain in U , the output trajectories satisfy $h(x_a(t)) \neq h(x_b(t))$ for some $t > 0$, i.e. the output trajectories are not identical.*

If we relax the condition and say that this holds when U is the entire space \mathcal{U} , then the system (2.1) is said to be observable at x_0 . If a system is (locally) observable at every x_0 , then it is said to be (locally) observable.

DEFINITION 2.2 (Accessibility). *Let $\mathcal{U} \subset \mathbb{R}^n$ be a set which contains some open ball with center $x = 0$. Let $\mathcal{R}(x(0), T)$ be the set (reachable set) containing all points \bar{x} for which there exists an input $u(\cdot) \in L^\infty([0, \infty); \mathbb{R}^m)$ such that the evolution of (2.1) from $x(0) \in \mathcal{U}$ satisfies $x(t) \in \mathcal{U}$ for $0 \leq t \leq T$ with $x(T) = \bar{x}$. The system (2.1) is said to be (locally) accessible if for all $x(0) \in \mathcal{U}$ the set $\bigcup_{t \leq T} \mathcal{R}(x(0), t)$ contains a non-empty open subset of \mathcal{U} for all $T > 0$.*

Throughout this article, we will assume that the system (2.1) is locally observable and locally accessible. We will also assume that the signal generator (2.2) is locally observable. From here, it is useful to establish definitions of Poisson stability and neutral stability of a system in connection to the signal generator.

DEFINITION 2.3 (Poisson stability). *A point $\omega_0 \in \mathbb{R}^d$ is said to be Poisson stable for system (2.2) if the flow $\Xi_t^s(\omega_0)$ generated by the vector field $s(\omega)$ is defined for all $t \in \mathbb{R}$ and, for each neighbourhood U^0 about ω_0 and each $T > 0$, there exists $t_1, t_2 \in \mathbb{R}$ with $t_1 > T$ and $t_2 < -T$, such that the flow satisfies $\Xi_{t_1}^s(\omega_0) \in U^0$ and $\Xi_{t_2}^s(\omega_0) \in U^0$.*

DEFINITION 2.4 (Neutral stability). *A dynamical system is said to be neutrally stable if $\omega = 0$ is a stable equilibrium, and there is an open neighbourhood W^0 around the origin in which every point is Poisson stable.*

Clearly, if the signal generator is neutrally stable on a domain W^0 , then $\omega(t)$ is persistent in time and does not decay to zero as time tends towards infinity, for any initial condition $\omega_0 \in W^0$. Furthermore, this implies that the linear approximation of the system around the origin $S = \left[\frac{\partial s}{\partial \omega} \right] \Big|_{\omega=0}$ has purely imaginary eigenvalues, and that these eigenvalues are semi-simple.

2.1. Notion of Moment. This paper focuses on the interconnected system (2.1)-(2.2) with the interconnection equation $u = v$. The interconnected system has a state-space representation given by

$$(2.4) \quad \begin{aligned} \dot{\omega} &= s(\omega), \\ \dot{x} &= f(x, \ell(\omega)), \\ y &= h(x), \\ \omega(0) &= \omega_0, \\ x(0) &= x_0. \end{aligned}$$

The notion of the time-domain moment for a nonlinear dynamical system comes from analyzing the steady-state output of the interconnected system given by (2.4) and makes use of the centre manifold theory. In order to help in our analysis of this interconnected dynamical system, we first define the notion of an invariant manifold and a centre manifold, which are introduced in more detail in [20], [13], [25].

DEFINITION 2.5 (Invariant Manifold). *Consider a system*

$$(2.5) \quad \dot{\xi} = \eta(\xi),$$

for $\xi \in \mathbb{R}^n$. A set \mathcal{M} is said to be an invariant manifold for (2.5) if $\xi(0) \in \mathcal{M} \Rightarrow \xi(t) \in \mathcal{M}$ for all $t \in \mathbb{R}$.

DEFINITION 2.6 (Centre Manifold). *Now consider a system of the form*

$$(2.6) \quad \begin{aligned} \dot{\omega} &= S\omega + \tilde{s}(\omega, x) \\ \dot{x} &= Ax + \tilde{f}(\omega, x), \end{aligned}$$

where $\omega(t) \in \mathbb{R}^d$, $x(t) \in \mathbb{R}^n$, S is a $(d \times d)$ matrix having all eigenvalues with zero real part, A is an $(n \times n)$ matrix having all eigenvalues with negative real part, and the functions \tilde{s} and \tilde{f} are C^2 with the functions and their first order derivatives vanishing at the origin. If $\mathcal{M} = \{(\omega, x) : x = \pi(\omega)\}$, for some function $\pi : \mathbb{R}^d \rightarrow \mathbb{R}^n$, is an invariant manifold for (2.6), it is also called a centre manifold if it is smooth with $\pi(0) = 0$ and $\frac{\partial \pi}{\partial \omega}(0) = 0$.

Moreover, the centre manifold \mathcal{M} characterized by the mapping $x = \pi(\omega)$ is said to be a locally attractive centre manifold for (2.6) if there exists a neighbourhood $U^0 \subset \mathbb{R}^d \times \mathbb{R}^n$ of $(0, 0)$ and constants $C \geq 1$, $\alpha > 0$ such that if $(\omega(0), x(0)) \in U^0$, then

$$(2.7) \quad \|x(t) - \pi(\omega(t))\| \leq Ce^{-\alpha t} \|x(0) - \pi(\omega(0))\|,$$

for all $t \geq 0$.

Under certain assumptions for the signal generator (2.2) and the system (2.1), we can assume that a locally attractive centre manifold exists between the two systems. We therefore make the following assumptions about the functions:

- (A1) The signal generator (2.2) is neutrally stable.
- (A2) The system (2.1) is locally exponentially stable in the first approximation about the equilibrium at the origin. That is, the matrix $A = \left[\frac{\partial f}{\partial x} \right] \Big|_{\substack{x=0 \\ u=0}}$ has only eigenvalues with negative real part.

The following result is a consequence of [20, Proposition 8.1.1]:

PROPOSITION 2.7. *Consider the interconnected system (2.4). If Assumptions (A1) and (A2) hold, then we are guaranteed the existence of a mapping $\pi : W^0 \subset \mathbb{R}^d \rightarrow \mathbb{R}^n$, defined on a neighbourhood W^0 about the origin, that characterizes a locally attractive centre manifold for (2.4). This mapping π satisfies, for all $\omega \in W^0$,*

$$(2.8) \quad \begin{aligned} \frac{\partial \pi}{\partial \omega}(\omega) s(\omega) &= f(\pi(\omega), \ell(\omega)), \\ \pi(0) &= 0. \end{aligned}$$

For each flow $\Xi_t^s(\omega_0)$ with initial condition $\omega_0 \in W^0$, the mapping π solving (2.8) produces a well-defined steady-state response in the interconnected system (2.4), given by

$$(2.9) \quad y_{ss}(t) = h(\pi(\Xi_t^s(\omega_0))).$$

Remark 2.8. Note that in the case where the system (2.1) and the signal generator (2.2) are both linear, with $s(\omega) = S\omega$, $\ell(\omega) = L\omega$ and $f(x, u) = Ax + Bu$, the invariance equation (2.8) simplifies to the well-known Sylvester equation

$$(2.10) \quad \Pi S = A\Pi + BL$$

where the matrix Π represents the invariant mapping $x = \Pi\omega$.

Because this centre manifold is locally attractive, (2.7) implies that for all initial conditions $\omega_0 \in W^0$, if the initial condition x_0 of the system is sufficiently close to the centre manifold, the output $y(t; \omega_0, x_0)$ generated by initial conditions (ω_0, x_0) satisfies

$$(2.11) \quad \lim_{t \rightarrow \infty} \|y(t; \omega_0, x_0) - h(\pi(\Xi_t^s(\omega_0)))\| = 0.$$

The steady-state response of the system is therefore defined by the invariant mapping between ω and x , which allows us to define what we mean by a system's moment.

DEFINITION 2.9 (Moment). *Assume that (2.8) has a solution π for the interconnected system (2.4). Then the time-domain moment of the interconnected system at (s, ℓ) is given by the function $h(\pi(\omega(\cdot)))$.*

Assumptions (A1) and (A2) guarantee that (2.8) has a solution, and that the notion of moment is in one-to-one relation with the steady-state output of the interconnected system (2.4) for initial conditions starting near the centre manifold \mathcal{M} . In the rest of the paper, we shall assume that assumptions (A1) and (A2) hold.

2.2. Moment-Based Reduced-Order Modeling. With the help of our previously defined notion of moment, we would like to use moment matching to develop a reduced-order model that is able to predict the long-term behaviour of the interconnected system, given a known signal generator input. The reduced-order model takes the form

$$(2.12) \quad \begin{aligned} \dot{r} &= \bar{f}(r, u) \\ y_r &= \bar{h}(r) \end{aligned}$$

with $r(t) \in \mathbb{R}^v$, with $v \ll n$, $u(t) \in \mathbb{R}^m$, and where \bar{f} is a C^2 mapping $\bar{f} : \mathbb{R}^v \times \mathbb{R}^m \rightarrow \mathbb{R}^v$ satisfying $\bar{f}(0, 0) = 0$. The output $y_r(t) \in \mathbb{R}^p$ is measured by the C^2 mapping $\bar{h} : \mathbb{R}^v \rightarrow \mathbb{R}^p$.

The goal is to construct a system of dimension $v \ll n$ whose output $y_r(t)$ matches the steady-state behaviour of $y(t)$ under the same signal generator input. We will use the following definition of a reduced-order model based on [3]:

DEFINITION 2.10. *The system described by (2.12) is a model at $s(\omega)$ of the system (2.1) if it has the same moment at $s(\omega)$ as (2.1). In this case, it is said to match the moment of the system at $s(\omega)$. Furthermore, system (2.12) is a reduced-order model of system (2.1) if it is a model at $s(\omega)$ of (2.1) and $v < n$.*

If the reduced-order model satisfies assumption (A2), then we know that there exists a mapping $p(\cdot)$ satisfying the equation

$$(2.13) \quad \begin{aligned} \frac{\partial p}{\partial \omega}(\omega) s(\omega) &= \bar{f}(p(\omega), \ell(\omega)) \\ p(0) &= 0. \end{aligned}$$

Under these assumptions, the steady-state output of (2.12) from an initial condition $\omega_0 \in W^0$, with r_0 sufficiently close to the centre manifold, satisfies

$$(2.14) \quad \lim_{t \rightarrow \infty} |y_r(t; \omega_0, r_0) - \bar{h}(p(\Xi_t^s(\omega_0)))| = 0.$$

Therefore, the reduced-order model (2.12) matches the moments of (2.1) at $s(\omega)$ if the mapping that solves (2.13) also satisfies

$$(2.15) \quad h(\pi(\omega)) = \bar{h}(p(\omega)).$$

Figure 1 depicts how moment matching corresponds to the matching of the steady-state responses of the full-order model and the reduced-order model.

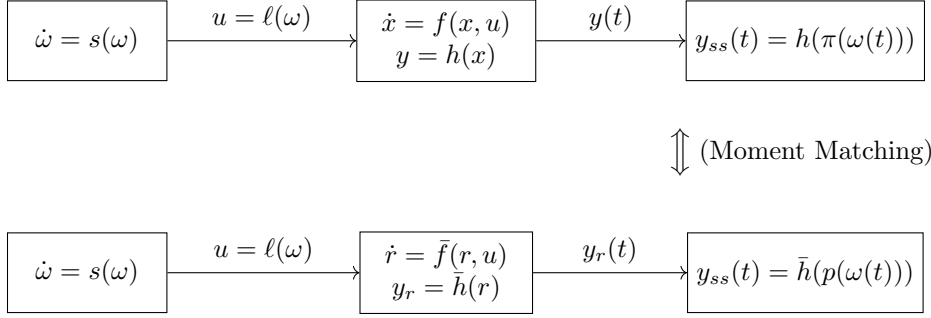


Fig. 1: Diagrammatic illustration of the concepts of moment matching in reduced-order modeling. The signal generator generates a control input to the high-order model and the reduced-order model, and moment-matching corresponds to the exact matching of their steady-state responses.

In order to construct a reduced-order model, we need to choose mappings \bar{f} and \bar{h} such that the equilibrium $(0,0)$ of \bar{f} is locally exponentially stable in the first approximation, and such that (2.13) and (2.15) hold. We note that choosing $p(\omega) = \omega$ and $\bar{h}(\omega) = h(\pi(\omega))$ allows the reduced-order model to satisfy (2.15), and as a consequence simplifies (2.13) to

$$(2.16) \quad s(\omega) = \bar{f}(\omega, \ell(\omega)).$$

In particular, it is shown in [4] that the choice of $p(\omega) = \omega$ gives us a family of reduced-order models

$$(2.17) \quad \begin{aligned} \dot{r} &= s(r) - \bar{g}(r, \ell(r)) + \bar{g}(r, u) \\ y_r &= h(\pi(r)) \end{aligned}$$

where the mapping \bar{g} is a free parameter, which can be chosen to ensure the local exponential stability about the origin of the autonomous system having dynamics given by

$$(2.18) \quad r \mapsto s(r) - \bar{g}(r, \ell(r)).$$

A suitable choice of \bar{g} can therefore ensure that Assumption (A2) holds, and that the reduced-order model given by (2.17) achieves moment matching.

It is convenient to have \bar{g} take the form $\bar{g}(r, \ell(r)) = g(r)\ell(r)$ for some C^2 mapping $g: \mathbb{R}^d \rightarrow \mathbb{R}^{d \times m}$. In the general case, one suitable mapping can be found by computing

$$(2.19) \quad S = \left[\frac{\partial s(r)}{\partial r} \right] \Big|_{(r=0)}, \quad L = \left[\frac{\partial \ell(r)}{\partial r} \right] \Big|_{(r=0)}$$

and choosing a mapping $g(r) = G$ for some real-valued matrix G such that $S - GL$ only has eigenvalues with negative real part, which can be accomplished if (S, L) is detectable. The linearization of (2.18) then simply becomes $S - GL$, and the assumption on the eigenvalues of $S - GL$ ensures that the system is locally exponentially stable.

3. Approximate solutions via Galerkin expansion. The main difficulty in constructing a reduced-order model by moment matching lies in obtaining a suitable mapping $\pi(\cdot)$ satisfying the PDE system

$$(3.1) \quad \begin{aligned} \frac{\partial \pi}{\partial \omega}(\omega) s(\omega) &= f(\pi(\omega), \ell(\omega)), \\ \pi(0) &= 0. \end{aligned}$$

A numerical scheme for approximating the solution to (3.1) is developed in this section.

3.1. Polynomial expansion of the invariant mapping. Proposition 2.7 only guarantees the existence of a solution to system (3.1) in a neighbourhood of the origin, hence we restrict our analysis to a compact domain $\Omega \subset \mathbb{R}^d$ containing the origin. We denote the i -th row of the n -dimensional mapping π by π_i , so $\pi(\omega) = (\pi_1(\omega), \pi_2(\omega), \dots, \pi_n(\omega))^\top$. For each mapping $\pi_i : \mathbb{R}^d \rightarrow \mathbb{R}$, $i=1, \dots, n$, we consider an expansion π_i^N of the form

$$(3.2) \quad \pi_i^N(\omega) = \sum_{k=1}^N c_{i,k} \phi_k(\omega) = \Phi^N(\omega) \mathbf{c}_i$$

where $\Phi^N = (\phi_1, \phi_2, \dots, \phi_N)$, and where $\{\phi_k\}_{k=1, \dots, N}$ satisfy $\phi_k \in C^\infty(\Omega)$ and belong to a complete family of basis functions in $H^1(\Omega)$. Note that we choose $H^1(\Omega)$ to ensure that $\frac{\partial \phi_i}{\partial \omega} \in L^2(\Omega)$. Here, $\mathbf{c}_i = (c_{i,1}, \dots, c_{i,k}, \dots, c_{i,N})^\top \in \mathbb{R}^N$ denotes the vector of coefficients associated with the basis functions ϕ_k for the i -th component of π . For this problem, we are interested in globally supported ansatz functions, such as monomials or orthogonal polynomials. The Galerkin residual method finds a weak solution to the invariant manifold π by projecting the mapping onto the space of functions $\{\phi_k\}$ and ensuring that the approximation error of the equation is orthogonal to every ϕ_j in the basis. The method of weighted residuals presented here and the resulting residual equations shown later are similar to those presented in [14] and [23].

The components of \mathbf{c}_i in (3.2) for $i = 1, \dots, n$ are found by setting the projection of the error in (3.1) to zero for all $\omega \in \Omega$ and imposing the Galerkin residual equation

$$(3.3) \quad \left\langle \frac{\partial \pi_i}{\partial \omega} s - f_i(\pi, \ell), \phi_j \right\rangle_\Omega = 0, \quad \text{for } j = 1, \dots, N$$

where the inner product is defined as

$$(3.4) \quad \langle f, g \rangle_\Omega = \int_\Omega f(\omega) g(\omega) d\omega.$$

We note that $\frac{\partial \pi_i}{\partial \omega}(\cdot) s(\cdot) - f_i(\pi(\cdot), \ell(\cdot)) \in L^2(\Omega)$ because π is smooth by the definition of the centre manifold, s and f are assumed to be at least C^2 , and Ω is compact.

For the sake of simplicity, based on the notation used in [7], with a slight abuse of notation we define the following extension of the inner product for vector-valued functions:

DEFINITION 3.1. *If $\eta : \mathbb{R}^N \rightarrow \mathbb{R}$ is a real-valued function, then we define*

$$(3.5) \quad \langle \eta, \Phi^N \rangle_\Omega = (\langle \eta, \phi_1 \rangle_\Omega, \dots, \langle \eta, \phi_N \rangle_\Omega)^\top.$$

If $\eta : \mathbb{R}^N \rightarrow \mathbb{R}^N$ is a real-valued function, then we define

$$(3.6) \quad \langle \eta, \Phi^N \rangle_\Omega = \begin{bmatrix} \langle \eta_1, \phi_1 \rangle_\Omega & \dots & \langle \eta_N, \phi_1 \rangle_\Omega \\ \vdots & & \vdots \\ \langle \eta_1, \phi_N \rangle_\Omega & \dots & \langle \eta_N, \phi_N \rangle_\Omega \end{bmatrix}.$$

In order to solve the nonlinear system (3.3), we introduce the high-dimensional function $F(\cdot) : \mathbb{R}^{Nn} \rightarrow \mathbb{R}^{Nn}$,

$$(3.7) \quad F(\mathbf{c}) := (F_1(\mathbf{c}), \dots, F_i(\mathbf{c}), \dots, F_n(\mathbf{c}))^\top$$

where each F_i is itself a multi-dimensional function $F_i : \mathbb{R}^{Nn} \rightarrow \mathbb{R}^N$, given by

$$(3.8) \quad F_i(\mathbf{c}) = \begin{bmatrix} \left\langle \frac{\partial \pi_i^N}{\partial \omega} s - f_i(\pi^N, \ell), \phi_1 \right\rangle_\Omega \\ \vdots \\ \left\langle \frac{\partial \pi_i^N}{\partial \omega} s - f_i(\pi^N, \ell), \phi_N \right\rangle_\Omega \end{bmatrix}.$$

By expanding π^N in this function, we express each F_i as a sum of linear and nonlinear components on \mathbf{c}_i . Using our notation for inner products, we can represent each $F_i(\cdot)$ as

$$(3.9) \quad F_i(\mathbf{c}) = \left\langle \frac{\partial \Phi^N}{\partial \omega} s, \Phi^N \right\rangle_\Omega \mathbf{c}_i - \left\langle f_i \left([\Phi^N \mathbf{c}_1, \dots, \Phi^N \mathbf{c}_n]^\top, \ell \right), \Phi^N \right\rangle_\Omega.$$

The linear term can be written as a matrix-vector product $\mathbf{A}\mathbf{c}$, where \mathbf{A} is defined as

$$(3.10) \quad \mathbf{A} = \left\langle \frac{\partial \Phi^N}{\partial \omega} s, \Phi^N \right\rangle_\Omega.$$

In order to deal with the second term in the right hand side of the expression, for convenience, we can define the function $G : \mathbb{R}^{Nn} \rightarrow \mathbb{R}^{Nn}$ as $G(\mathbf{c}) = (G_1(\mathbf{c}), \dots, G_n(\mathbf{c}))^\top$ with

$$(3.11) \quad G_i(\mathbf{c}) = - \left\langle f_i \left([\Phi^N \mathbf{c}_1, \dots, \Phi^N \mathbf{c}_n]^\top, \ell \right), \Phi^N \right\rangle_\Omega.$$

Using this notation, we can then write F_i as

$$(3.12) \quad F_i(\mathbf{c}) = \mathbf{A}\mathbf{c}_i + G_i(\mathbf{c})$$

and the overall function as

$$(3.13) \quad F(\mathbf{c}) = \mathbf{A} \begin{bmatrix} \mathbf{c}_1 \\ \vdots \\ \mathbf{c}_n \end{bmatrix} + G(\mathbf{c}).$$

Remark 3.2. If the function f determining the system's dynamics is a polynomial of sufficiently low degree, for example if it is linear, quadratic, or cubic in π , the functions G_i can be represented with matrices and tensors similar to \mathbf{A} . In problems where this is the case, it will be useful to construct a matrix or tensor representation of the function in order to accelerate both assembly and iterative computations.

In order to find the coefficients \mathbf{c} satisfying $F(\mathbf{c}) = 0$, we employ a Newton iteration, which iterates until $\|F(\mathbf{c})\|_1$ is below a given tolerance. To carry out this iteration, we also need to find the Jacobian of the Galerkin residual function. The

Jacobian is defined as $JF : \mathbb{R}^{Nn} \rightarrow \mathbb{R}^{Nn \times Nn}$, with $JF(\mathbf{c}) = \frac{\partial F}{\partial \mathbf{c}}(\mathbf{c})$. Based on our formulation in (3.9), we represent it as

$$(3.14) \quad JF(\mathbf{c}) = \begin{bmatrix} JF_{1,1}(\mathbf{c}) & \dots & JF_{n,1}(\mathbf{c}) \\ \vdots & & \vdots \\ JF_{1,n}(\mathbf{c}) & \dots & JF_{n,n}(\mathbf{c}) \end{bmatrix}$$

where the corresponding entries are given by

$$(3.15) \quad JF_{i,j}(\mathbf{c}) = \delta_{ij}\mathbf{A} + \frac{\partial G_i}{\partial \mathbf{c}_j}(\mathbf{c}).$$

Here, δ_{ij} denotes the Kronecker delta acting on the indices i and j . The functions $\frac{\partial G_i}{\partial \mathbf{c}_j}$ can be computed using the chain rule:

$$(3.16) \quad \frac{\partial G_i}{\partial \mathbf{c}_j}(\mathbf{c}) = - \left\langle \frac{\partial f_i(\pi^N, \ell)}{\partial \mathbf{c}_j} \Phi^N, \Phi^N \right\rangle_{\Omega} \Big|_{\pi^N = \Phi^N \mathbf{c}}.$$

Based on the expression of $F(\mathbf{c})$ in (3.9) and of $JF(\mathbf{c})$ in (3.15), we calculate the Newton increment $\Delta \mathbf{c}^k$ by solving

$$(3.17) \quad JF(\mathbf{c}^k)\Delta \mathbf{c}^k = F(\mathbf{c}^k),$$

and the Newton update is then

$$(3.18) \quad \mathbf{c}^{k+1} = \mathbf{c}^k - \Delta \mathbf{c}^k.$$

Remark 3.3. Note that in some cases, depending on the system dynamics under study, the Jacobian JF may become singular. In these scenarios, we solve for the Newton increment $\Delta \mathbf{c}^k$ in the least-squares sense.

3.2. Polynomial basis. The construction of the polynomial basis for our approximation largely follows the procedure used in [23, Section 4.1]. In order to construct the basis functions to be used in the Galerkin approximation over the d -dimensional space Ω , we first select a maximum degree M and construct a basis in a single scalar variable ω up to the degree M . We denote this basis by $\varphi_M : \mathbb{R} \rightarrow \mathbb{R}^M$. In our case, we will use the monomial basis

$$(3.19) \quad \varphi_M(\omega) = (\omega, \omega^2, \dots, \omega^M).$$

Note that, since our invariance equation (3.1) specified that $\pi(0) = 0$, we do not require a constant term in our basis. In this paper we are using a monomial basis but in general, it is possible to use the same generation method based on a different chosen one-dimensional basis, for example orthogonal bases such as Legendre or Chebyshev polynomials up to degree M .

In order to generate the multi-dimensional basis, we use the tensor product of the basis in each coordinate and eliminate those terms whose total degree is higher than the prescribed maximum degree M . The basis is then given by

$$(3.20) \quad \Phi^N = \left\{ \phi \in \bigotimes_{j=1}^d \varphi_M(\omega_j), \text{ where } \deg(\phi) \leq M \right\}.$$

The number of basis functions N is combinatorially related to the maximum degree M . A stars-and-bars argument is used to count the number of monomials of a given total degree, and the summation over all degrees up to M can be evaluated in closed form using the hockey-stick identity, yielding

$$(3.21) \quad N = \sum_{m=1}^M \binom{d+m-1}{m} = \binom{M+d}{M} - 1.$$

In our case, where the one-dimensional basis is just given as the monomials up to degree M , each basis polynomial ϕ_i can be conveniently written as the separable function

$$(3.22) \quad \phi_i(\omega) = \prod_{j=1}^d \phi_i^j(\omega_j) = \prod_{j=1}^d \omega_j^{\nu_{i,j}} \quad \text{where} \quad \sum_{j=1}^d \nu_{i,j} \leq M$$

for exponents $\nu_{i,j}$.

3.3. Integration. We are concerned with the assembly of \mathbf{A} , G_i , and $\frac{\partial G_i}{\partial \mathbf{c}_j}$. Each component of $\mathbf{A} = \left\langle \frac{\partial \Phi^N}{\partial \omega} s, \Phi^N \right\rangle_{\Omega}$ is given by

$$(3.23) \quad \mathbf{A}_{i,j} = \left\langle \frac{\partial \phi_j}{\partial \omega} s, \phi_i \right\rangle_{\Omega} = \sum_{k=1}^d \int_{\Omega} \frac{\partial \phi_j}{\partial \omega_k}(\omega) s_k(\omega) \phi_i(\omega) d\omega,$$

where $s(\omega) = (s_1(\omega), \dots, s_d(\omega))^{\top}$. When each $s_k(\omega)$ is a monomial, this expression can be computed exactly. Each component of $G_i(\mathbf{c}) = -\langle f_i(\pi^N, \ell), \Phi^N \rangle_{\Omega}$ is represented as

$$(3.24) \quad G_i(\mathbf{c})_j = -\langle f_i(\pi^N, \ell), \phi_j \rangle_{\Omega} = -\int_{\Omega} f_i(\pi^N(\omega), \ell(\omega)) \phi_j(\omega) d\omega,$$

and is approximated using a suitable quadrature rule, for example Gauss-Legendre quadrature in d dimensions over Ω . The entries of $\frac{\partial G_i}{\partial \mathbf{c}_j} = -\left\langle \frac{\partial f_i(\pi^N, \ell)}{\partial \mathbf{c}_j} \Phi^N, \Phi^N \right\rangle_{\Omega}$ are computed analogously,

$$(3.25) \quad \left[\frac{\partial G_i}{\partial \mathbf{c}_j} \right]_{k,l} = -\left\langle \frac{\partial f_i(\pi^N, \ell)}{\partial \mathbf{c}_j} \phi_l, \phi_k \right\rangle_{\Omega} = -\int_{\Omega} \frac{\partial f_i(\pi^N(\omega), \ell(\omega))}{\partial \mathbf{c}_j} \phi_l(\omega) \phi_k(\omega) d\omega,$$

and are likewise approximated by a suitable quadrature rule.

3.4. Computational complexity and implementation. The bulk of the computation comes from integration over d dimensions to evaluate the function F and its Jacobian JF as well as the computation of the Newton update $\Delta \mathbf{c}^k$. The computational complexity of integration scales exponentially with d unless f and s are separable or have exploitable structure, as discussed in Remark 3.2; in such cases the integral can be handled via approximations such as the Monte Carlo method.

When the integrals admit an analytical solution, evaluating F has complexity $O(Nn)$ and evaluating JF has complexity $O(N^2n^2)$. Solving $JF(\mathbf{c}^k) \Delta \mathbf{c}^k = F(\mathbf{c}^k)$ via a direct or least-squares solver has cubic complexity in Nn , though in many cases JF is sparse, which significantly reduces this cost. Overall, the computational cost depends on the system dimension n and combinatorially on the signal generator dimension d and maximum degree M .

4. Numerical results. Different numerical experiments are performed to assess the approximation quality of the Galerkin method and the performance of the resulting reduced-order models. The tests are carried out over rectangular domains Ω of varying sizes, for different nonlinear dynamics and signal generators, and the algorithm is employed with a tolerance of 10^{-7} in the L^1 norm of F . In each case, the solver is initialized with $\mathbf{c}^0 = \mathbf{0}$, with all coefficients of π^N set to zero.

The quality of the Galerkin approximation is measured via the residual error function $R = (R_1, \dots, R_n)^\top$, where for each $i = 1, \dots, n$ the residual at a specified ω is given by

$$(4.1) \quad R_i(\mathbf{c}, \omega) = \frac{\partial \pi_i^N}{\partial \omega}(\omega) s(\omega) - f_i(\pi^N(\omega), \ell(\omega)).$$

To quantify the approximation quality globally, we compute the L_2 norm of each R_i averaged over a chosen test domain W ,

$$(4.2) \quad \|R_i\|_{(2,W)} = \sqrt{\int_W |R_i(\mathbf{c}, \omega)|^2 d\omega},$$

and aggregate these into a single metric weighted by the relative magnitude of the coefficients \mathbf{c}_i :

$$(4.3) \quad \|R\|_{(2,W)} = \frac{\sum_{i=1}^n \|\mathbf{c}_i\|_2 \|R_i\|_{(2,W)}}{\sum_{i=1}^n \|\mathbf{c}_i\|_2}.$$

When a reduced-order model can be constructed, its performance is assessed by comparing steady-state outputs. Given time series $y_k = y(t_k)$ and $y_{r,k} = y_r(t_k)$ sampled at times $\{t_k\}_{k=1}^K$, we identify a time T_{ss} beyond which both models have reached steady state, and set $k_s = \min\{k : t_k \geq T_{ss}\}$. Denoting by $\frac{1}{2}(\max_{k \geq k_s} y_k - \min_{k \geq k_s} y_k)$ the signal amplitude in steady state, the relative RMS error is

$$(4.4) \quad \epsilon_{rel} = \frac{\left(\frac{1}{K_s} \sum_{k=k_s}^K \|y_{r,k} - y_k\|_2^2\right)^{1/2}}{\frac{1}{2}(\max_{k \geq k_s} y_k - \min_{k \geq k_s} y_k)},$$

where $K_s = K + 1 - k_s$ is the number of samples in the steady-state regime.

Three examples are considered. The first, in [Subsection 4.1](#), serves as a proof of concept on a low-dimensional nonlinear system for which an analytical solution is known, demonstrating the algorithm's ability to recover exact solutions when the components of π belong to the span of the basis. The second and third examples, in [Subsection 4.2](#) and [Subsection 4.3](#), consider a high-dimensional system of dimension $n = 1000$ driven by a linear and a nonlinear signal generator respectively, demonstrating scalability and the ability to construct accurate reduced-order models in the absence of an analytical solution.

4.1. Test 1: Cart pendulum. First, we consider the position control of a nonlinear cart pendulum, based on a problem studied in [\[32, Section 3.2\]](#). The signal generator is chosen by selecting target dynamics for the cart pendulum with $d = 2$ and $n = 4$. The dynamics of the interconnected system are governed by

$$s(\omega) = \begin{bmatrix} \omega_2 \\ \frac{a_1 \sin(\omega_1)}{1 + k a_2 \cos(\omega_1)} \end{bmatrix}, \quad \ell(\omega) = \frac{k a_1 \sin(\omega_1)}{1 + k a_2 \cos(\omega_1)}, \quad k < -\frac{1}{a_2}$$

$$f(x, u) = \begin{bmatrix} x_3 \\ x_4 \\ a_1 \sin(x_1) - a_2 \cos(x_1)u \\ u \end{bmatrix}, \quad h(x) = x_1 \quad a_1 > 0, a_2 > 0.$$

This problem admits the analytical solution

$$\pi(\omega) = (\omega_1, k\omega_1, \omega_2, k\omega_2)^\top.$$

The function F and its Jacobian JF take the form

$$F(\mathbf{c}) = \begin{bmatrix} \mathbf{A}\mathbf{c}_1 - \mathbf{M}\mathbf{c}_3 \\ \mathbf{A}\mathbf{c}_2 - \mathbf{M}\mathbf{c}_4 \\ \mathbf{A}\mathbf{c}_3 - H(\mathbf{c}_1) \\ \mathbf{A}\mathbf{c}_4 - \gamma \end{bmatrix}, \quad JF(\mathbf{c}) = \begin{bmatrix} \mathbf{A} & 0 & -\mathbf{M} & 0 \\ 0 & \mathbf{A} & 0 & -\mathbf{M} \\ -\frac{\partial H}{\partial \mathbf{c}_1} & 0 & \mathbf{A} & 0 \\ 0 & 0 & 0 & \mathbf{A} \end{bmatrix}$$

using the previously defined matrix \mathbf{A} in (3.23), as well as the matrices and vectors

$$(4.5) \quad \mathbf{M} = \langle \Phi^N, \Phi^N \rangle_\Omega, \quad \mathbf{P} = \langle \Phi^N \omega_1, \Phi^N \rangle_\Omega, \quad \gamma = \langle \ell(\omega), \Phi^N \rangle_\Omega,$$

and the function $H : \mathbb{R}^N \rightarrow \mathbb{R}^N$ given by

$$H(\mathbf{c}_1) = \langle a_1 \sin(\Phi^N \mathbf{c}_1) - a_2 \cos(\Phi^N \mathbf{c}_1) \ell(\omega), \Phi^N \rangle_\Omega \\ \frac{\partial H}{\partial \mathbf{c}_1} = \langle \Phi^N (a_1 \cos(\Phi^N \mathbf{c}_1) + a_2 \sin(\Phi^N \mathbf{c}_1) \ell(\omega)), \Phi^N \rangle_\Omega.$$

Due to the choice of $s(\omega)$, the matrix \mathbf{A} is singular and consequently JF is also singular; Newton iteration updates are therefore computed in the least-squares sense. Using the constants $a_1 = 2$, $a_2 = 3$, and $k = -\frac{2}{3}$, Table 1 shows that the method achieves near-exact recovery of the analytical solution over $\Omega = [-1, 1]^2$. The solution admits a monomial representation and the algorithm recovers it to within the prescribed numerical tolerance, with observed errors on the order of 10^{-9} .

	$M = 2$	$M = 4$	$M = 6$	$M = 8$
$\ R(\mathbf{c}, \omega)\ _{(2, W)}$	9.3×10^{-10}	8.6×10^{-10}	9.4×10^{-10}	2.4×10^{-9}
Time (s)	0.83	16.8	135	646

Table 1: Residual error $\|R(\mathbf{c}, \omega)\|_{(2, W)}$ and computational time for the Galerkin approximation of the invariant mapping π for Test 1.

4.2. Test 2: Nonlinear resistor-inductor ladder with linear oscillator as signal generator. We consider the nonlinear resistor-inductor (RL) ladder, based on a slightly modified version of the circuit schematic in [34, Figure 7] and also considered in [24] in a model order reduction context. The signal generator has dimension $d = 2$ and the system has a repeating structure admitting any state dimension n . The signal generator is given by

$$(4.6) \quad s(\omega) = \begin{bmatrix} 0 & a \\ -a & 0 \end{bmatrix} \begin{bmatrix} \omega_1 \\ \omega_2 \end{bmatrix}, \quad \ell(\omega) = \omega_2, \quad a \in \mathbb{R} \setminus \{0\}$$

and the system dynamics are

$$(4.7) \quad \begin{bmatrix} \dot{x}_1 \\ \dot{x}_2 \\ \vdots \\ \dot{x}_{n-1} \\ \dot{x}_n \end{bmatrix} = \underbrace{\begin{bmatrix} -2\kappa & 1 & & & \\ 1 & -2\kappa & 1 & & \\ & \ddots & \ddots & \ddots & \\ & & & 1 & -2\kappa & 1 \\ & & & & 1 & -2\kappa \end{bmatrix}}_{=: f(x, u)} \begin{bmatrix} x_1 \\ x_2 \\ \vdots \\ x_{n-1} \\ x_n \end{bmatrix} - \begin{bmatrix} x_1^2/2 + x_1^3/3 \\ x_2^2/2 + x_2^3/3 \\ \vdots \\ x_{n-1}^2/2 + x_{n-1}^3/3 \\ x_n^2/2 + x_n^3/3 \end{bmatrix} + \begin{bmatrix} 1 \\ 0 \\ \vdots \\ 0 \\ 0 \end{bmatrix} u$$

$$h(x) = x_1.$$

The parameter $\kappa = 1$ renders the system unstable beyond a certain dimension n ; we therefore use $\kappa = 1.1$ throughout. Since the nonlinearities in each f_i are polynomials of degree 2 and 3 depending only on x_i , the construction of F and JF admits the following simplifications. We introduce the tensors

$$(4.8) \quad \begin{aligned} \mathbf{N} &\in \mathbb{R}^{N \times N \times N}, [\mathbf{N}]_{i,j,k} = \int_{\Omega} \phi_i \phi_j \phi_k d\omega \\ \mathbf{O} &\in \mathbb{R}^{N \times N \times N \times N}, [\mathbf{O}]_{i,j,k,l} = \int_{\Omega} \phi_i \phi_j \phi_k \phi_l d\omega, \end{aligned}$$

and the matrix-valued functions $\mathcal{N} : \mathbb{R}^N \rightarrow \mathbb{R}^{N \times N}$ and $\mathcal{O} : \mathbb{R}^N \rightarrow \mathbb{R}^{N \times N}$,

$$(4.9) \quad [\mathcal{N}(\mathbf{v})]_{i,j} = \sum_{k=1}^N v_k N_{i,j,k}, \quad [\mathcal{O}(\mathbf{v})]_{i,j} = \sum_{k=1}^N \sum_{l=1}^N v_k v_l O_{i,j,k,l}.$$

Defining $P, Q : \mathbb{R}^N \rightarrow \mathbb{R}^{N \times N}$ as

$$(4.10) \quad \begin{aligned} P(\mathbf{v}) &= \left(\mathbf{A} + 2\kappa \mathbf{M} + \frac{1}{2} \mathcal{N}(\mathbf{v}) + \frac{1}{3} \mathcal{O}(\mathbf{v}) \right) \mathbf{v} \\ Q(\mathbf{v}) &= \mathbf{A} + 2\kappa \mathbf{M} + \mathcal{N}(\mathbf{v}) + \mathcal{O}(\mathbf{v}), \end{aligned}$$

where \mathbf{A} and \mathbf{M} are as in (3.23) and (4.5), the function F and its Jacobian take the form

$$(4.11) \quad F_i(\mathbf{c}) = P(\mathbf{c}_i) - (1 - \delta_{i,1}) \mathbf{M} \mathbf{c}_{i-1} - (1 - \delta_{i,n}) \mathbf{M} \mathbf{c}_{i+1} - \delta_{i,1} \boldsymbol{\gamma},$$

where $\boldsymbol{\gamma}$ is the same as in (4.5), and $\delta_{i,j}$ denotes the Kronecker delta, and

$$(4.12) \quad JF(\mathbf{c}) = \begin{bmatrix} Q(\mathbf{c}_1) & -\mathbf{M} & & & \\ -\mathbf{M} & Q(\mathbf{c}_2) & -\mathbf{M} & & \\ & \ddots & \ddots & \ddots & \\ & & & -\mathbf{M} & Q(\mathbf{c}_{n-1}) & -\mathbf{M} \\ & & & & -\mathbf{M} & Q(\mathbf{c}_n) \end{bmatrix}.$$

Computing the tensors \mathbf{N} and \mathbf{O} exactly rather than by numerical quadrature allows for a significant reduction in computational cost by exploiting the structure of the system dynamics.

The method is validated on a full-order model with $n = 1000$ and $a = 2$, over the domain $\Omega = [-0.6, 0.6]^2$, with residual errors measured on $W = \Omega$. The choice of domain is discussed further in [Subsection 5.1](#). The residual errors $\|R(\mathbf{c}, \omega)\|_{(2,W)}$ reported in [Table 2](#) show that increasing M systematically improves the approximation, as expected from the nested structure of the polynomial spaces. The small residual errors at higher degrees suggest that $[-0.6, 0.6]^2$ lies within the neighbourhood W^0 over which π is well-defined, and that π^N converges to the weak solution of the invariance equation as the number of basis functions increases.

To construct the reduced-order model, we recall from [\(2.17\)](#) the family of models

$$\begin{aligned}\dot{r} &= s(r) - \bar{g}(r, \ell(r)) + \bar{g}(r, u) \\ y_r &= h(\pi(r)),\end{aligned}$$

where $\bar{g}(\cdot)$ is a free mapping to be chosen to ensure local exponential stability. For this system, the choice

$$(4.13) \quad \bar{g}(r, u) = \begin{bmatrix} 0 \\ c \end{bmatrix} u$$

achieves local exponential stability for any $c > 0$. To verify this, we examine the linearization about the origin of $\frac{\partial}{\partial r} \left(s(r) - \begin{bmatrix} 0 \\ c \end{bmatrix} \ell(r) \right)$, whose eigenvalues are those of $\begin{bmatrix} 0 & a \\ -a & -c \end{bmatrix}$, which have strictly negative real part for all $c > 0$. The reduced-order model is then

$$(4.14) \quad \begin{aligned}\dot{r} &= s(r) - \begin{bmatrix} 0 \\ c \end{bmatrix} \ell(r) + \begin{bmatrix} 0 \\ c \end{bmatrix} u \\ y_r &= h(\pi^N(r)),\end{aligned}$$

for the approximate solution π^N to the invariant mapping. [Figure 2a](#) shows the outputs $y(t)$ and $y_r(t)$ for $n = 1000$, $M = 6$, $\Omega = [-0.6, 0.6]^2$, $c = 10$, and initial conditions $\omega_0 = (0.2, 0.2)^\top$, $r_0 = (0, 1)^\top$, $x_0 = 0$, over $t \in [0, 30]$. The relative RMS error ϵ_{rel} , defined in [\(4.4\)](#) and reported in [Table 2](#), is on the order of 10^{-3} across all values of M , confirming that the reduced-order model accurately reproduces the full-order steady-state output despite the large dimensionality reduction.

4.3. Test 3: Nonlinear resistor-inductor ladder with Van der Pol oscillator as signal generator. We now consider the same RL ladder system [\(4.7\)](#) driven by the Van der Pol oscillator as signal generator,

$$(4.15) \quad s(\omega) = \begin{bmatrix} \omega_2 \\ -\omega_1 + \mu(1 - \omega_1^2)\omega_2 \end{bmatrix} \quad \ell(\omega) = \omega_2 \quad \mu > 0.$$

The tensors \mathbf{N} and \mathbf{O} from [Test 2](#) are reused; only \mathbf{A} is reconstructed using $s(\omega)$ in [\(4.15\)](#), and the expressions [\(4.11\)](#)–[\(4.12\)](#) for F_i and JF remain unchanged.

The invariance equation is solved with $\mu = 1$, $\kappa = 1.1$, over $\Omega = W = [-0.6, 0.6]^2$ for $n = 1000$. The residual errors in [Table 2](#) confirm that higher polynomial degree yields better approximations, and that the method remains tractable under nonlinear excitation.

For the reduced-order model, we use the mapping

$$(4.16) \quad \bar{g}(r, u) = \begin{bmatrix} 0 \\ \mu(1 - r_1^2) + c \end{bmatrix} u,$$

yielding the reduced-order model

$$(4.17) \quad \begin{aligned} \dot{r} &= s(r) - \begin{bmatrix} 0 \\ \mu(1 - r_1^2) + c \end{bmatrix} \ell(r) + \begin{bmatrix} 0 \\ \mu(1 - r_1^2) + c \end{bmatrix} u \\ y_r &= h(\pi^N(r)). \end{aligned}$$

Local exponential stability follows from the linearization of

$$\frac{\partial}{\partial r} \left(s(r) - \begin{bmatrix} 0 \\ \mu(1 - r_1^2) + c \end{bmatrix} \ell(r) \right)$$

about the origin, which gives the matrix $\begin{bmatrix} 0 & 1 \\ -1 & -c \end{bmatrix}$, whose eigenvalues have negative real part for all $c > 0$.

Figure 2b shows the model outputs for $n = 1000$, $M = 6$, $c = 10$, and initial conditions $\omega_0 = (0.2, 0.2)^\top$, $r_0 = (0, 1)^\top$, $x_0 = 0$, over $t \in [0, 30]$. The relative RMS errors ϵ_{rel} in Table 2 decrease monotonically with M , confirming that the polynomial basis has sufficient representational capacity to capture the nonlinear steady-state behaviour induced by the Van der Pol excitation.

		$M = 2$	$M = 4$	$M = 6$	$M = 8$
$\ R(\mathbf{c}, \omega)\ _{(2,W)}$	Test 2	3.4×10^{-4}	1.9×10^{-6}	2.0×10^{-8}	6.5×10^{-10}
	Test 3	7.4×10^{-3}	2.0×10^{-4}	1.2×10^{-5}	8.1×10^{-7}
ϵ_{rel}	Test 2	4.6×10^{-3}	4.5×10^{-3}	4.5×10^{-3}	4.5×10^{-3}
	Test 3	1.7×10^{-1}	7.0×10^{-2}	4.9×10^{-2}	4.1×10^{-2}

Table 2: Galerkin approximation results for the RL ladder system ($n = 1000$): residual error $\|R(\mathbf{c}, \omega)\|_{(2,W)}$ of the invariant mapping π and relative steady-state RMS error ϵ_{rel} of the reduced-order model, for Test 2 (linear oscillator) and Test 3 (Van der Pol signal generator).

5. Discussion of Results. The numerical results of the previous section demonstrate that the proposed method achieves moment matching and accurately recovers the steady-state output of the full-order model. The residual analysis confirms convergence of the polynomial approximation to the weak solution of the invariance equation with increasing degree. This section provides additional numerical evidence and examines the behaviour of the method under parameter variations, with all experiments based on the RL ladder driven by the Van der Pol oscillator from Subsection 4.3, with the same constants and initial conditions.

5.1. Effect of domain and nonlinearities. The mapping π is only theoretically guaranteed to exist in a neighbourhood W^0 of the origin, and the polynomial approximation π^N is constructed over a chosen domain Ω . The size of Ω therefore directly affects both the approximation quality of π^N and whether the mapping satisfying (3.1) is well-defined over that domain. Larger domains amplify higher-order monomials near the boundary and can magnify small coefficient errors.

Figure 3 illustrates this for $\mu = 0.25$, $\mu = 1$, and $\mu = 2$, corresponding to increasingly nonlinear regimes of the Van der Pol signal generator, with residuals measured

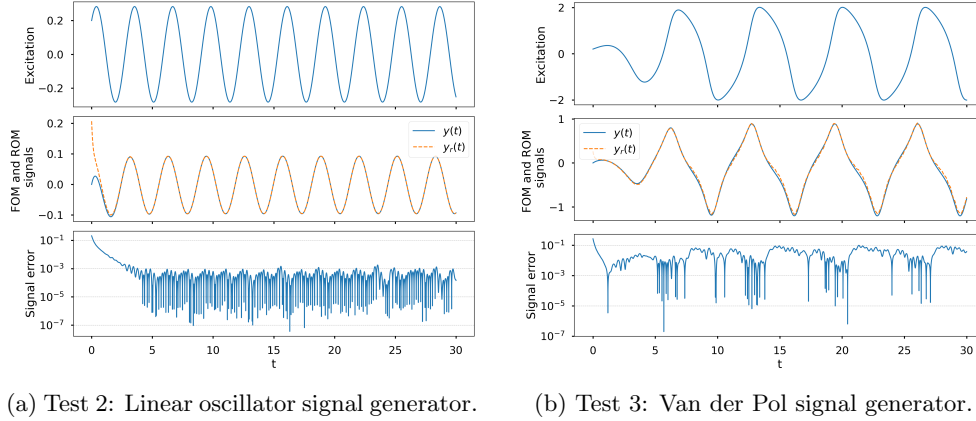


Fig. 2: Time evolution of the excitation signal $\omega_1(t)$, the full-order output $y(t)$, the reduced-order output $y_r(t)$, and the error $|y(t) - y_r(t)|$ for the RL ladder system ($n = 1000$) over $t \in [0, 30]$.

on $W = [-0.6, 0.6]^2$. The results confirm that the choice of Ω has a significant effect on approximation quality, and that increased signal generator nonlinearity heightens sensitivity to the domain. This is attributable to the cubic term $\mu\omega_1^2\omega_2$ in the nonlinearity, which grows rapidly near the boundary when Ω or μ are large, thereby amplifying small coefficient errors in the approximate mapping π^N . Despite this, the method maintains stable convergence and acceptable accuracy across the tested parameter range for moderate domain sizes.

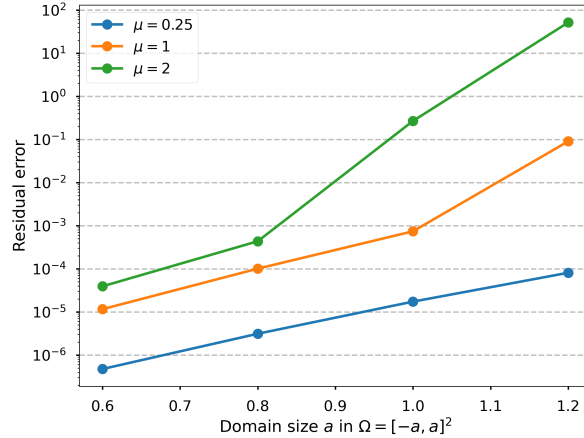


Fig. 3: PDE residual error as a function of domain size Ω for different values of the nonlinearity constant μ in the Van der Pol oscillator signal generator for Test 3. The tests were carried out with a maximum degree $M = 6$ for the problem with $n = 1000$ dimensions and constants $\kappa = 1.1$, $c = 10$, and tested on $W = [-0.6, 0.6]^2$.

5.2. Comparison to other ROM techniques. To provide a benchmark, the proposed method is compared against Proper Orthogonal Decomposition (POD) [42] and Balanced Truncation (BT) [38], two established linear model reduction techniques that do not exploit the structured interconnection or nonlinear excitation present in the considered systems. The implementations are described as follows.

For POD, snapshots of the full-order state $x(t)$ were collected by simulating a single trajectory with an initial condition varying from the one tested, over the time interval $t \in [0, 50]$ with initial conditions $\omega_0 = (0.1, 0.3)^\top$ and $x_0 = 0$. The snapshot matrix was assembled from 500 uniformly spaced time samples and the POD basis was extracted via a truncated singular value decomposition retaining $r = 2$ modes. The reduced dynamics were obtained by Galerkin projection of the full nonlinear system onto the POD subspace.

For BT, the method was applied to the system linearized about the origin. The controllability and observability Gramians were computed analytically by solving the associated Lyapunov equations, and the system was truncated to retain $r = 2$ states. The input and output matrices B and C were taken from the linearization of f and h , respectively.

For Test 3 with $M = 8$ and reduced dimension $r = 2$, the proposed method achieves $\epsilon_{rel} = 4.1 \times 10^{-2}$, compared to 5.7×10^{-2} for POD and 1.2×10^{-1} for BT. Figure 4 further illustrates the advantage of moment matching through phase portrait comparisons: the state trajectory reconstructed via π^N more closely follows that of the full-order model than either POD or BT at the same reduced dimension.

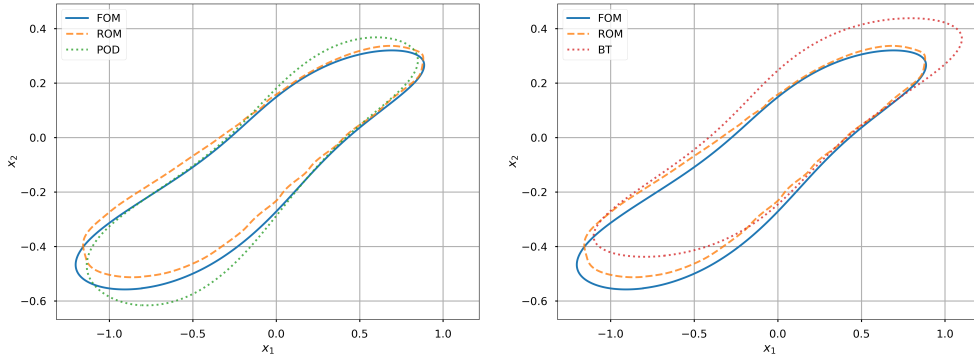


Fig. 4: Phase portraits of the full-order model (x_1, x_2) and approximate mapping $(\pi_1(\omega), \pi_2(\omega))$ for Test 3, contrasted with the POD ROM (left) and the BT ROM (right).

5.3. Computational complexity. Table 3 reports the number of basis functions N , Newton iterations, and total computation time for Test 3. The Jacobian JF is stored sparsely, so the time complexity scales linearly in n and quadratically in N . The rapid convergence of both the residual and RMS error with M means that $M = 4$ or $M = 6$ already provides a good approximation at manageable cost.

Regarding online cost, for $t = 50$, $n = 1000$, and $r = 2$, the FOM requires 0.4243 seconds to simulate while the ROM requires 0.0120 seconds, a speedup of $35.3\times$. This arises from integrating an r -dimensional system rather than the full n -dimensional one, with $r \ll n$, with the evaluation of π^N at the final time adding a cost that

	$M = 2$	$M = 4$	$M = 6$	$M = 8$
N	5	14	27	44
Iterations	3	3	3	3
Time (s)	1.92	80	1065	8423

Table 3: Number of basis functions N , Newton iterations, and total computational time for the Galerkin approximation of π in Test 3.

scales with N . For the offline computation, the tensors \mathcal{N} and \mathcal{O} have sizes $O(N^3)$ and $O(N^4)$ respectively; explicit storage was feasible for the problems considered here, though symmetry-based compression or on-demand computation could be employed if storage becomes prohibitive. The Jacobian JF and function evaluation F have sizes $O(N^2)$ and $O(N)$ respectively, while the coefficients of π^N require $O(nN)$ storage online.

5.4. Concluding remarks. This paper presents a numerical framework for approximating the solution of the invariance PDE system arising in nonlinear moment matching. A Galerkin expansion through a polynomial basis yields an approximate invariant mapping π^N that can be used to construct reduced-order models accurately reproducing the steady-state output of systems with state dimension up to $n = 1000$. Computational efficiency is achieved by exploiting the problem structure through pre-computed matrix and tensor representations.

Nonlinear moment matching is most applicable when the dominant behaviour of a high-dimensional system is governed by a low-dimensional driving subsystem. In this setting, the reduced-order model evolves in a low-dimensional space while the nonlinear complexity of the full-order system is encoded in the mapping π . Despite the breadth of the theoretical moment matching literature, computational methods for solving the invariance equation in high dimensions have been lacking; this paper addresses that gap directly.

This moment matching method improves upon both POD and BT, and its underlying invariance PDE formulation extends naturally beyond model reduction to output regulation and immersion and invariance design. Future work will address signal generators of higher dimensionality, enabling reduced-order models for richer input regimes while requiring new strategies to manage the associated computational challenges.

6. Code and Data Availability. The code used to generate the numerical results in this paper is publicly available and can be viewed on GitHub at: <https://github.com/carlosjdoebeli/Moment-Matching-ROM>.

REFERENCES

- [1] A. ANTOUNAS, *An overview of approximation methods for large-scale dynamical systems*, Annual Reviews in Control, 29 (2005), pp. 181–190, <https://doi.org/10.1016/j.arcontrol.2005.08.002>.
- [2] A. C. ANTOUNAS, *Approximation of Large-Scale Dynamical Systems*, Society for Industrial and Applied Mathematics, 2005, <https://doi.org/10.1137/1.9780898718713>.
- [3] A. ASTOLFI, *Model reduction by moment matching for nonlinear systems*, in 2008 47th IEEE Conference on Decision and Control, 2008, pp. 4873–4878, <https://doi.org/10.1109/CDC.2008.4738791>.

- [4] A. ASTOLFI, *Model reduction by moment matching for linear and nonlinear systems*, IEEE Transactions on Automatic Control, 55 (2010), pp. 2321–2336, <https://doi.org/10.1109/TAC.2010.2046044>.
- [5] A. ASTOLFI AND R. ORTEGA, *Immersion and invariance: a new tool for stabilization and adaptive control of nonlinear systems*, IEEE Transactions on Automatic Control, 48 (2003), pp. 590–606, <https://doi.org/10.1109/TAC.2003.809820>.
- [6] B. AZMI, D. KALISE, AND K. KUNISCH, *Optimal feedback law recovery by gradient-augmented sparse polynomial regression*, Journal of Machine Learning Research, 22 (2021), pp. 1–32, <http://jmlr.org/papers/v22/20-755.html>.
- [7] R. W. BEARD, *Improving the Closed-Loop Performance of Nonlinear Systems*, PhD thesis, Rensselaer Polytechnic Institute, 1995.
- [8] R. W. BEARD, G. N. SARIDIS, AND J. T. WEN, *Galerkin approximations of the generalized Hamilton-Jacobi-Bellman equation*, Automatica, 33 (1997), pp. 2159–2177, [https://doi.org/10.1016/S0005-1098\(97\)00128-3](https://doi.org/10.1016/S0005-1098(97)00128-3).
- [9] R. BELLMAN, *Adaptive Control Processes: A Guided Tour*, Princeton University Press, 1961, <http://www.jstor.org/stable/j.ctt183ph6v> (accessed 2023-10-27).
- [10] P. BENNER AND P. GOYAL, *Interpolation-based model order reduction for polynomial parametric systems*, 2019, <https://arxiv.org/abs/1904.11891>.
- [11] P. BENNER, W. SCHILDERS, S. GRIVET-TALOCIA, A. QUARTERONI, G. ROZZA, AND L. MIGUEL SILVEIRA, *Model Order Reduction: Volume 3 Applications*, De Gruyter, 2020, <https://doi.org/10.1515/9783110499001>.
- [12] C. I. BYRNES AND A. ISIDORI, *Limit sets, zero dynamics, and internal models in the problem of nonlinear output regulation*, IEEE Transactions on Automatic Control, 48 (2003), pp. 1712–1723.
- [13] J. CARR, *Applications of Centre Manifold Theory*, Springer-Verlag New York Inc., 1981, <https://doi.org/10.1007/978-1-4612-5929-9>.
- [14] N. FAEDO, G. SCARCIOTTI, A. ASTOLFI, AND J. V. RINGWOOD, *On the approximation of moments for nonlinear systems*, IEEE Transactions on Automatic Control, 66 (2021), pp. 5538–5545, <https://doi.org/10.1109/TAC.2021.3054325>.
- [15] K. GALLIVAN, A. VANDENDORPE, AND P. VAN DOOREN, *Sylvester equations and projection-based model reduction*, Journal of Computational and Applied Mathematics, 162 (2004), pp. 213–229, <https://doi.org/10.1016/j.cam.2003.08.026>. Proceedings of the International Conference on Linear Algebra and Arithmetic 2001.
- [16] W. GRAY AND J. SCHERPEN, *Nonlinear Hilbert adjoints: properties and applications to Hankel singular value analysis*, in Proceedings of the 2001 American Control Conference., vol. 5, 2001, pp. 3582–3587, <https://doi.org/10.1109/ACC.2001.946190>.
- [17] W. GRAY AND E. VERRIEST, *Balanced realizations near stable invariant manifolds*, Automatica, 42 (2006), pp. 653–659, <https://doi.org/10.1016/j.automatica.2005.12.007>.
- [18] R. HERMANN AND A. KRENER, *Nonlinear controllability and observability*, IEEE Transactions on Automatic Control, 22 (1977), pp. 728–740, <https://doi.org/10.1109/TAC.1977.1101601>.
- [19] T. C. IONESCU AND A. ASTOLFI, *Nonlinear moment matching-based model order reduction*, IEEE Transactions on Automatic Control, 61 (2015), pp. 2837–2847.
- [20] A. ISIDORI, *Nonlinear Control Systems*, Springer London, 3 ed., 1995, <https://doi.org/10.1007/978-1-84628-615-5>.
- [21] A. ISIDORI AND C. I. BYRNES, *Steady-state behaviors in nonlinear systems with an application to robust disturbance rejection*, Annual Reviews in Control, 32 (2008), pp. 1–16, <https://doi.org/10.1016/j.arcontrol.2008.01.001>.
- [22] D. KALISE, S. KUNDU, AND K. KUNISCH, *Robust feedback control of nonlinear PDEs by numerical approximation of high-dimensional Hamilton-Jacobi-Isaacs equations*, 2019, <https://arxiv.org/abs/1905.06276>.
- [23] D. KALISE AND K. KUNISCH, *Polynomial approximation of high-dimensional hamilton-jacobi-bellman equations and applications to feedback control of semilinear parabolic pdes*, SIAM Journal on Scientific Computing, 40 (2017), <https://doi.org/10.1137/17M1116635>.
- [24] Y. KAWANO AND J. M. SCHERPEN, *Empirical differential gramians for nonlinear model reduction*, Automatica, 127 (2021), p. 109534, <https://doi.org/10.1016/j.automatica.2021.109534>.
- [25] H. KHALIL, *Nonlinear Systems*, Always Learning, Pearson, 2015, <https://books.google.co.uk/books?id=Gt2HAQAACAAJ>.
- [26] B. KRAMER, S. GUGERCIN, AND J. BORGGAARD, *Nonlinear balanced truncation: Part 2 – model reduction on manifolds*, 2023, <https://arxiv.org/abs/2302.02036>.
- [27] B. KRAMER, S. GUGERCIN, J. BORGGAARD, AND L. BALICKI, *Nonlinear balanced truncation:*

- Part 1-computing energy functions*, 2022, <https://arxiv.org/abs/2209.07645>.
- [28] K. KUNISCH AND S. VOLKWEIN, *Control of the Burgers equation by a reduced-order approach using proper orthogonal decomposition*, Journal of Optimization Theory and Applications, 102 (1999), pp. 345–371, <https://api.semanticscholar.org/CorpusID:118949739>.
- [29] K. KUNISCH AND S. VOLKWEIN, *Proper orthogonal decomposition for optimality systems*, ESAIM: Mathematical Modelling and Numerical Analysis, 42 (2008), pp. 1–23, <http://eudml.org/doc/250374>.
- [30] A. MORESCHINI AND A. ASTOLFI, *Closed-loop interpolation by moment matching for linear and nonlinear systems*, IEEE Transactions on Automatic Control, (2025), <https://doi.org/10.1109/TAC.2024.3484309>. (Early Access).
- [31] A. MORESCHINI, M. SCANDELLA, AND T. PARISINI, *Nonlinear data-driven moment matching in Reproducing Kernel Hilbert Spaces*, in European Control Conference (ECC), 2024, pp. 3440–3445, <https://doi.org/10.23919/ECC64448.2024.10590737>.
- [32] R. ORTEGA, B. YI, J. G. ROMERO, AND A. ASTOLFI, *Orbital stabilization of nonlinear systems via the immersion and invariance technique*, International Journal of Robust and Nonlinear Control, 30 (2020), pp. 1850–1871, <https://doi.org/10.1002/rnc.4861>.
- [33] D. RAFIQ AND M. A. BAZAZ, *Model order reduction via moment-matching: A state of the art review*, Archives of Computational Methods in Engineering, (2022), <https://doi.org/10.1007/s11831-021-09618-2>.
- [34] M. REWIENSKI AND J. WHITE, *A trajectory piecewise-linear approach to model order reduction and fast simulation of nonlinear circuits and micromachined devices*, IEEE Transactions on Computer-Aided Design of Integrated Circuits and Systems, 22 (2003), pp. 155–170, <https://doi.org/10.1109/TCAD.2002.806601>.
- [35] G. SCARCIOTTI AND A. ASTOLFI, *Data-driven model reduction by moment matching for linear and nonlinear systems*, Automatica, 79 (2017), pp. 340–351, <https://doi.org/https://doi.org/10.1016/j.automatica.2017.01.014>.
- [36] G. SCARCIOTTI AND A. ASTOLFI, *Interconnection-based model order reduction-a survey*, European Journal of Control, 75 (2024), p. 100929.
- [37] J. SCHERPEN AND W. GRAY, *Minimality and local state decompositions of a nonlinear state space realization using energy functions*, IEEE Transactions on Automatic Control, 45 (2000), pp. 2079–2086, <https://doi.org/10.1109/9.887630>.
- [38] J. M. A. SCHERPEN, *Balancing for nonlinear systems*, Systems & Control Letters, 21 (1993), pp. 143–153.
- [39] J. D. SIMARD, A. MORESCHINI, AND A. ASTOLFI, *Parameterization of all moment matching interpolants*, in European Control Conference (ECC), 2023, pp. 1–6, <https://doi.org/10.23919/ECC57647.2023.10178406>.
- [40] J. D. SIMARD, A. MORESCHINI, AND A. ASTOLFI, *Parameterization of all differential-algebraic moment matching interpolants*, IEEE Transactions on Automatic Control, (2024), <https://doi.org/10.1109/TAC.2024.3469247>. (Early Access).
- [41] H. J. SUSSMANN AND V. JURDJEVIC, *Controllability of nonlinear systems*, Journal of Differential Equations, 12 (1972), pp. 95–116, [https://doi.org/10.1016/0022-0396\(72\)90007-1](https://doi.org/10.1016/0022-0396(72)90007-1), <https://www.sciencedirect.com/science/article/pii/0022039672900071>.
- [42] K. WILLCOX AND J. PERAIRE, *Balanced model reduction via the proper orthogonal decomposition*, AIAA Journal, 40 (2002), pp. 2323–2330, <https://doi.org/10.2514/2.1570>.